

# Modelling and Simulation of Medium Temperature Latent Heat Thermal Energy Storage System

Anurag Gupta\*, Manoj Kumar\*\*

\* (Faculty of Engineering, Dayalbagh Educational Institute (Deemed to be University), Agra, India)

\*\* (Department of Mechanical Engineering, Dayalbagh Educational Institute (Deemed to be University), Agra)

## ABSTRACT

In the pursuit of uninterrupted power supply, energy storage systems have become indispensable, particularly during nighttime when solar energy is unavailable. Among various energy storage methods, Latent Heat Thermal Energy Storage (LHTES) systems stand out due to their high energy density and isothermal operation. This paper presents the modelling and simulation of a latent heat thermal energy storage system (LHTES) using a phase change material (PCM) in steady state. A comprehensive LHTES design has been developed in SolidWorks 2021, incorporating Erythritol as the chosen PCM. This novel design methodology aims to size the LHTES for a 1 MJ capacity, integrating principles of thermodynamics, heat transfer, and fluid mechanics. Through mathematical modelling and simulation in Ansys Workbench and Fluent, various parameters are analysed in steady state for the 1 MJ LHTES, including temperature profiles within the hot oil (high tech therm. 66) and temperature distribution in the radial and axial directions of the inner and outer tubes. This research advances the understanding and design of Latent Heat Thermal Energy Storage (LHTES) systems, contributing to the sustainable and efficient utilization of thermal energy.

**Keywords**—LHTES, PCM, Erythritol, Simplec

Date of Submission: 10-10-2023

Date of acceptance: 24-10-2023

## I. Introduction

All humans on earth have a variety of fundamental requirements. Such requirements are satisfied by equipment or machines, which save time and money and reduce human effort. These machines provide human beings with comfort, and all machines and equipment require electricity for power. On Earth, there are two categories of energy sources: 1.) Non-renewable energy sources and 2.) Renewable energy sources. Non-renewable energy sources are those energy sources that are derived directly from nature and do not require conversion for use, such as coal, natural gas, oil, and nuclear energy; however, these energy sources are limited on earth and deplete over time. According to data from world coal statistics, 1,139,471,430,000 tonnes of coal have been stored for 133 years[1]. According to world oil reserves, there are 1,650,585,140,000 barrels of crude remaining on the planet. Oil consumption is 35,442,913,090 barrels per year, or 97,103,871 barrels per day; therefore, according to these figures, oil is only reserved for the next 47 years[2]. Likewise, there are only

692,922,220,000 million cubic feet of natural gas left, which is enough for 52 years[3]. Consequently, renewable energy is the only energy source that completely satisfies this demand on earth. Numerous types of renewable energy, such as wind energy, ocean energy, hydroelectricity energy, and thermal energy, etc., are found on the planet, and this renewable energy total satisfies the demand for energy in terms of supply. We can convert wind energy into electricity, ocean tidal energy into hydropower, and hydropower into energy. However, only solar energy can be readily converted into electricity. Therefore, we only focus on solar energy, which is not available at night. It is only available in day. Or it is unavailable during overcast or rainy weather. Therefore, thermal energy storage will be required for energy storage.

There are primarily three varieties of thermal energy storage systems: 1.) Sensible energy storage system (such as liquid and solid types), 2.) Latent heat thermal energy storage system (such as solid liquid or liquid solid types), and 3.) Chemical energy storage system.

The focus of my research pertains only to the Latent Heat Thermal Energy Storage (LHTES) system. Consequently, the advantages and disadvantages of LHTES (Latent Heat Thermal Energy Storage System) are delineated as follows:

#### **Benefits of Latent Heat Thermal Energy Storage [LHTES]**

- **High energy storage density:** By using phase change materials (PCM) that absorb or release latent heat during a phase transition (such as the solid-liquid transition), LHTES can store a lot of energy in a little amount of space.
- **Compact in size:** Compared to other energy storage technologies, LHTES systems can be built to have a comparatively modest physical footprint.
- LHTES can be linked with renewable energy sources like solar and wind to store extra energy produced under favourable conditions for later consumption.
- **Waste Heat Recovery (WHR):** Using LHTES, waste heat from industrial processes can be collected and stored, making it accessible for later use or to enhance.

#### **Disadvantages of Latent Heat Thermal Energy Storage (LHTES)**

- **Discretionary temperature range:** LHTES (Latent heat thermal energy storage systems) are normally made for temperature ranges. Because of this restriction, they might not be appropriate for uses that call for a wide range of operating temperatures. They might not be appropriate for industrial procedures involving high temperatures, for instance.
- **Material compatibility:** Materials with phase-change properties are needed for LHTES (Latent heat thermal energy storage systems). The technology's application may be constrained by the difficulty of locating suitable materials that can endure repeated phase changes without degrading.
- **Limitations of heat transmission:** Especially during the phase-change process, heat transfer in LHTES (Latent heat thermal energy storage systems). devices can be relatively slow. Due to the lengthier charging and discharging durations, the system may be less sensitive to changes in energy demand.
- **Size and volume requirements:** To accommodate the storage materials and related equipment, LHTES (Latent heat thermal energy storage systems). systems frequently need a sizable

amount of space. In applications with limited space, this may be a drawback.

Reviews of latent heat storage products and systems for various temperatures and uses have been published in significant numbers. In several of them, LHTES for CSP applications is discussed. Reviews of the various storage methods and storage materials [SHTES, LHTES, and TCTES] for high temperature CSP applications were presented by Gil et al. [2010] and Medrano et al. [2010]. For solar applications above 300 °C, LHTES was evaluated by Cárdenas and León in 2013 and Liu et al. in 2012. A review of PCM for solar applications with a temperature range of 120–1000 °C was published by Kenisarin [2010], along with information on the thermos physical characteristics of possible materials including salt compositions and metal alloys. A review of solid-liquid phase change materials by Zalba et al. [2003] that concentrated on materials, heat travel, and applications. Additionally, several reviews about solar cooling applications have been presented; most of them [Brancato et al., 2017, Khan et al., 2017] examined latent heat storage below 150 °C, except for Pintaldi et al. [2015], whose review of LHTES media and systems reached PCM with melting temperatures as high as 250 °C. Also published were reviews of PCM for solar heating applications [Mahfuz et., 2014], solar water tanks with PCM layers [Jabbar et al., 2013], and solar water heating systems with PCM floors [Huang et al., 2014]. Reviews of PCM utilised in buildings or for automotive applications [Cabeza et al., 2011; Jaguemont et al., 2018] have also been carried out.

There are also more thermal energy storage methods, including molten salt storage and thermochemical energy storage, each with their own benefits and drawbacks. The precise needs and limitations of the intended application determine the best thermal energy storage method[4].

This study evaluates potential phase change materials (PCMs) for a waste heat transportation system (TH system) using DSC and TG-DTA. Erythritol emerges as the optimal PCM due to its high latent heat, thermal stability, and chemical durability, making it suitable for the TH system. Notably, heat release tests reveal foaming behaviour and encapsulation of oil droplets within solidified erythritol during contact with cold oil. For detailed explanation and graphs of the study kindly consider reference [5].

This research examines the suitability of sugar alcohols as phase change materials (PCMs) for thermal energy storage between 70-180 °C. The study investigates five pure sugar alcohols, three

eutectic blends, and evaluates their melting points, latent heats of fusion, and key physical properties across temperatures. Comparison with conventional PCMs and potential applications, like solar seasonal energy storage, are also addressed[6].

This study investigates the thermal stability of erythritol, a promising organic phase change material (PCM). It assesses the impact of thermal treatment on erythritol's properties and aims to enhance its stability. The research finds that erythritol's latent heat degradation follows a first-order reaction, and mixing it with an antioxidant reduces degradation, promoting thermal stability, particularly under argon atmosphere[7].

Sugar alcohols are studied as phase transition materials for long-term heat storage, focusing on nucleation and crystal growth kinetics, interfacial free energy, latent heat, and viscosity. Combining theoretical calculations and experimental studies. Molecular dynamic simulations using a generalised AMBER force field offer thermodynamic properties, whereas tests evaluate heat capacity, viscosity, and crystal growth kinetics. The study shows how high viscosity and interfacial free energy slow sugar alcohol nucleation and crystal development [8].

Erythritol was used as the PCM and a heat-transfer oil to study the heat release capabilities of a direct-contact heat exchanger. Agyenim et al. evaluated whether erythritol could be used to power a LiBr/H<sub>2</sub>O absorption cooling system and the best parameters for charging and discharging it[9].

A direct-contact heat exchanger with erythritol PCM and heat-transfer oil is tested for heat release. A vertical cylinder HSU with a downward nozzle is used. Optimising HTO flow rate and PCM layer height affects heat-released temperature efficacy, rate, and volumetric heat transfer coefficient. Heat transfer efficiency, temperature effectiveness, and heat release rate increase with steady HTO flow. Direct-contact heat exchangers efficiently release PCM latent heat, especially with uniform HTO flow[10].

**Table 1:** Thermo-physical properties of high-tech therm 66.

| Property                        | High tech therm66     |
|---------------------------------|-----------------------|
| Density @ (150 °C)              | 921 kg/m <sup>3</sup> |
| Specific heat @ (150 °C)        | 2015 J/kg * K         |
| Thermal conductivity @ (150 °C) | 0.109 W/m K           |
| Viscosity @ (150 °C)            | 1.52 MPa s            |

## II. Modelling and Analysis

### 2.1 Physical Design

According to the calculation, done in accordance with the flow diagram Fig 1, we have found out the Radius of inner tube (R1), Radius of intermediate tube (R2), Radius of outer tube (R3), and length of tubes (L),[11] of triple tube heat exchanger for the novel designing methodology. The radius of inner tube is 25mm and radius of intermediate tube is 38.54 mm and radius of outer tube is 46.54 mm, and the thickness of all tube is 1mm. the LHTES used three tubes which are made by steel. Inner tubes and outer tubes used for flowing hot oil (High tech therm 66) at 150 ° C. And intermediate tube used for holding the PCM (erythritol) 1350 cm<sup>3</sup> volume according to 1MJ capacity. TABLE 1 [12] illustrates the physical properties of Heat Transfer Fluid whereas TABLE 2 [13][14] illustrates the Thermo-physical properties of PCM and Steel Tube.

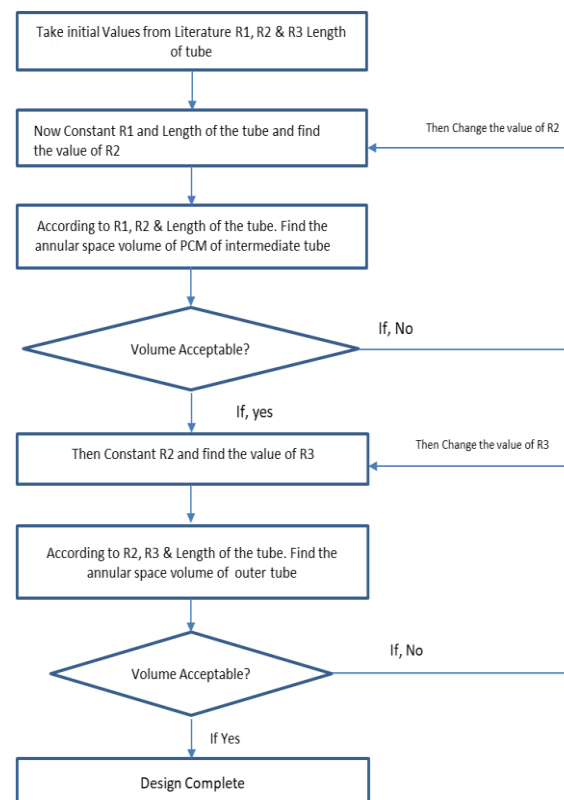


Fig 1: flow diagram of novel design methodology of LHTES.

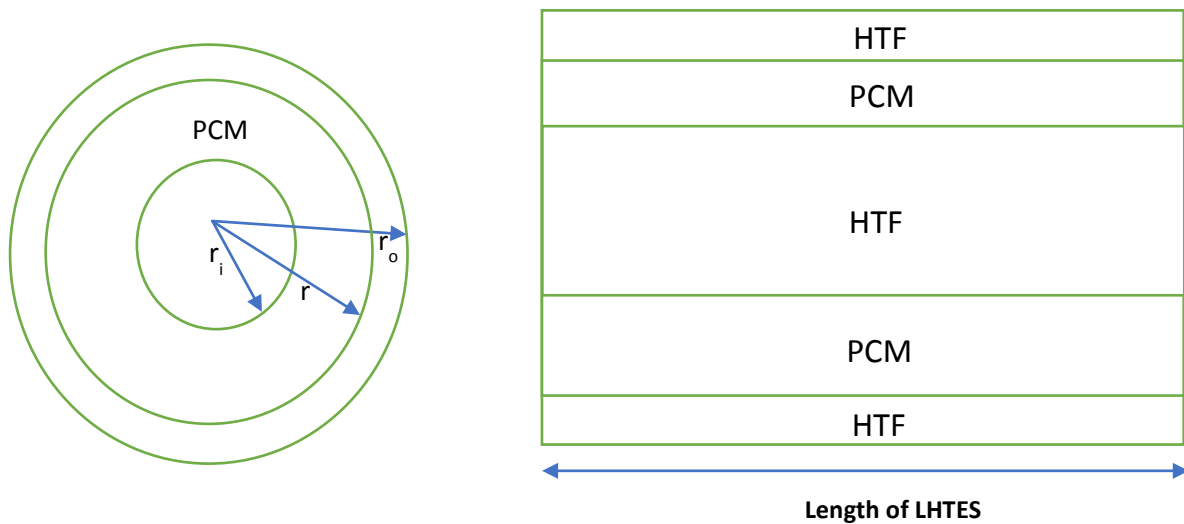


Fig 2: depicts the physical setup of the LHTES model.

## 2.2 Governing Equations

Our thermal energy storage system has three concentric tubes: inner tube, intermediate tube and outer tube. In inner tube and outer tube, hot oil is flowing at 150 °C. and an intermediate tube is filled with PCM. When hot oil flows in tubes then oil heat transfers in to PCM. Therefore, we can store the thermal energy from oil in to PCM and this thermal energy will convert into desired form and use it. This system works like an open system. So,

enthalpy entering in the system is  $h_1$  and enthalpy leaving from the system is  $h_2$ . We can easily find out the change in enthalpy  $\Delta H$ .

$$\dot{Q} = M_{\text{inner tube}} C_p (T_i - T_f)$$

$T_i$  (inlet initial Temperature of hot oil in inner tube) = 150°C

$C_p$  (Specific heat of oil) @ 150 °C = 1.52 MPa s

$\dot{m}$  (mass flow rate) of hot oil in inner tube = 0.04605 kg/s.

$Q$  (500 KJ/hour) = 0.1388 KJ/s

Table 2: Thermo-physical properties of PCM and Steel Tube.

| Property  | Erythritol                | Steel                     |
|---|---------------------------|---------------------------|
| Density of PCM, solid $\rho_s$ (20 °C)                  | 1480 (Kg/m <sup>3</sup> ) | 8030 (Kg/m <sup>3</sup> ) |
| Density of PCM liquid $\rho_l$ (140 °C)                 | 1300 (Kg/m <sup>3</sup> ) |                           |
| Melting point of PCM                                    | 118°C                     |                           |
| Latent heat of PCM                                      | 339.9 (KJ/Kg)             |                           |
| Thermal conductivity in solid state ( $k_s$ ) (20 °C)   | 0.733 (W/m K)             | 16.27 (W/m K)             |
| Thermal conductivity in liquid state ( $k_l$ ) (140 °C) | 0.326 (W/m K)             |                           |
| $C_p$ in solid state (20 °C)                            | 1.38 KJ/Kg K              | 502.48 (J/Kg K)           |
| $C_p$ in liquid state (140 °C)                          | 2.76 KJ/Kg K              |                           |
| Dynamic viscosity ( $\mu$ )                             | 0.01 Kg/ms                |                           |
| Thermal expansion coefficient                           | 0.001014 1/K              |                           |
| Temperature solidus ( $T_s$ )                           | 389.85 K                  |                           |
| Temperature liquidus ( $T_s$ )                          | 391.85 K                  |                           |

The governing equations underpinning physics should always be examined before beginning a CFD simulation. The governing equations are the same as any other fluids problem, even if we have additional complexity factors like pulsatile flow and non-Newtonian fluids. The continuity equation and the Navier-Stokes equations are the two most basic governing equations. Here, let's quickly go over the equations. When represented in cylindrical coordinates, the continuity equation from the first equation looks like this with assumptions steady flow and incompressible flow:[15]

$$\frac{1}{r} \frac{\partial(rV_r)}{\partial r} + \frac{1}{r} \frac{\partial(V_\theta)}{\partial \theta} + \frac{\partial(V_z)}{\partial z} = 0$$

The Navier-Stokes equations given in the second equation can be expressed in cylindrical coordinates as with assumptions constant density and viscosity:

$$\rho \left( v_r \frac{\partial v_r}{\partial r} + \frac{v_\theta}{r} \frac{\partial v_r}{\partial \theta} + v_z \frac{\partial v_r}{\partial z} \right) = -\frac{\partial p}{\partial r} + \mu \left[ \frac{1}{r} \frac{\partial}{\partial r} \left( r \frac{\partial v_r}{\partial r} \right) + \frac{1}{r^2} \frac{\partial^2 v_r}{\partial \theta^2} + \frac{\partial^2 v_r}{\partial z^2} \right] + \rho g_r$$

$$\rho \left( v_r \frac{\partial v_\theta}{\partial r} + \frac{v_\theta}{r} \frac{\partial v_\theta}{\partial \theta} + v_z \frac{\partial v_\theta}{\partial z} - \frac{v_\theta^2}{r} \right) = -\frac{\partial p}{\partial r} + \mu \left[ \frac{\partial}{\partial r} \left( \frac{1}{r} \frac{\partial}{\partial r} (r v_\theta) \right) + \frac{1}{r^2} \frac{\partial^2 v_\theta}{\partial \theta^2} + \frac{\partial^2 v_\theta}{\partial z^2} - \frac{2}{r^2} \frac{\partial v_\theta}{\partial \theta} \right] + \rho g_\theta$$

$$\rho \left( v_r \frac{\partial v_z}{\partial r} + \frac{v_\theta}{r} \frac{\partial v_z}{\partial \theta} + v_z \frac{\partial v_z}{\partial z} + \frac{v_r v_\theta}{r} \right) = -\frac{\partial p}{\partial z} + \mu \left[ \frac{\partial}{\partial r} \left( \frac{1}{r} \frac{\partial}{\partial r} (r v_\theta) \right) + \frac{1}{r^2} \frac{\partial^2 v_\theta}{\partial \theta^2} + \frac{\partial^2 v_\theta}{\partial z^2} + \frac{2}{r^2} \frac{\partial v_r}{\partial \theta} \right] + \rho g_z$$

### 2.3 Initial and Boundary Conditions

Latent heat thermal energy storage has the initial and boundary conditions for simulate the model in Ansys fluent at the initial condition PCM was solid at 27°C and heat transfer fluid (high tech therm 66) at 150 °C. At the inlet of the Inner and outer tube the boundary condition of latent heat thermal energy storage are as follows:

#### Inside heating method

$$\text{at } r = r_i \rightarrow T = T_{HTF} ;$$

$$\text{at } r = r_m \rightarrow \frac{\partial T}{\partial r} = 0$$

#### Heating both sides method

$$\text{at } r = r_i \rightarrow T = T_{HTF} = 423 \text{ K}$$

$$\text{at } r = r_m \rightarrow T = T_{HTF} = 423 \text{ K}$$

$$\text{at } r = r_0 \rightarrow q = 0 = T = \text{constant.}$$

#### Initial temperature for all models

$$\text{at } t = 0 \rightarrow T = T_{ini}$$

### 2.4 Grid Independence Testing

Grid independence testing was done on Domain Nodes elements at 1807127.

The domain Nodes description is given below:

| Domain                  | Elements |         |
|-------------------------|----------|---------|
| Inner pipe solid        | 40160    | 20000   |
| Intermediate pipe solid | 26400    | 13120   |
| Outer pipe solid        | 21920    | 10880   |
| Part fluid              | 185299   | 928546  |
| Part PCM                | 161784   | 834581  |
| All Domains             | 435563   | 1807127 |

### 2.5 Numerical Modelling

Geometry of LHTES has been modelled in Ansys workbench in design modeler. According to dimension which is calculated. After that Geometry has been meshed in mesh section in Ansys fluent. Mesh size 0.002 mm mesh type is tetrahedron. After modelling and meshing of LHTES in Ansys design modeler after that same modelling simulated in Ansys fluent at following parameter with constant thermophysical properties of PCM such as specific heat, thermal conductivity, viscosity.

GENERAL: Pressure based solver which is used for incompressible flow [16] in steady state, and the algorithm used for this simulation is simple and is described by Patanker [17] to solve the pressure velocity coupling.

MODEL: Energy on, Laminar.

MATERIALS: a) High tech therm66 @150°C (thermic fluid oil in inner tube and outer tube)

b)PCM @ 25°C (erythritol)

BOUNDARY CONDITIONS: a) Velocity inlet:0.025477m/s @ 150°C

b) Pressure outlet

SOLUTION METHOD: Simplex Method

SOLUTION INITIALIZATION: Standard Initialization

RUN CALCULATION: 1000 Iteration

After the simulation we get Velocity contour and Temperature contour.

### III. Result and Discussions

Temperature contours are shown in Fig 3, and velocity contours are shown in Fig 4 for the hot oil that is contained within the inner and outer tubes. After running a simulation, it becomes clear that in the XY plane along the axis, ranging from 1mm to 500mm, as shown in Fig 5, temperature contours change fast within the first 10.5mm. This is illustrated by the fact that the axis ranges from 1mm to 500mm. The heat that was transferred from the hot oil to the phase change material (PCM) is responsible for the quick transformation that occurred.

When compared to the first 400 millimetres of the entry length, the heat transfer considerably slows down once it passes the 10.5mm mark. Isothermal lines begin to become visible within the PCM at the 400-mm mark and continue to grow in length until they reach the 500-mm mark. These isothermal lines can only be seen along the tube's axis inside the outermost 5 mm of the tube's circumference. They indicate that there has been a decrease in the temperature of the PCM at the end of the outer tube, which is a change that is predominantly driven by external conditions.

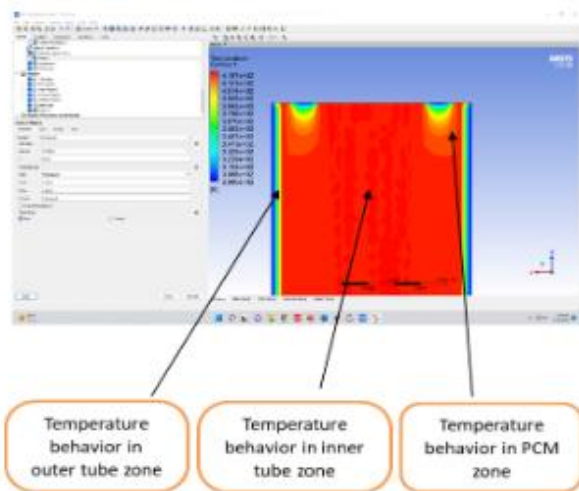


Fig 3: temperature contour

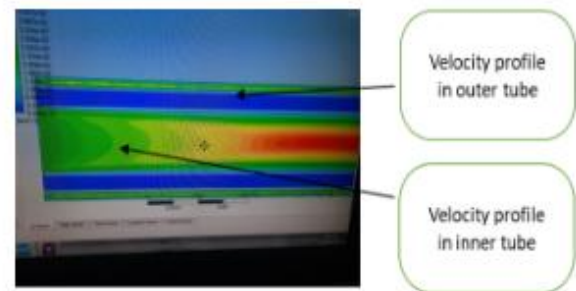
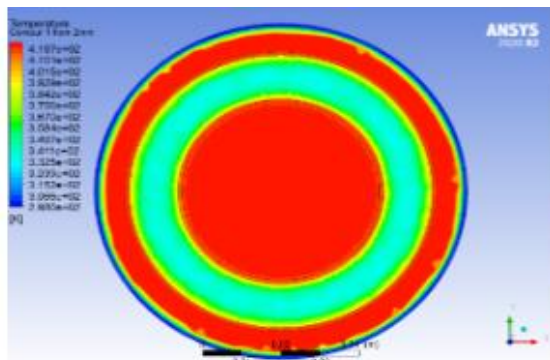
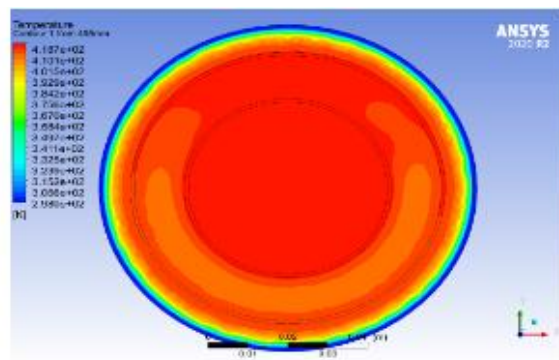


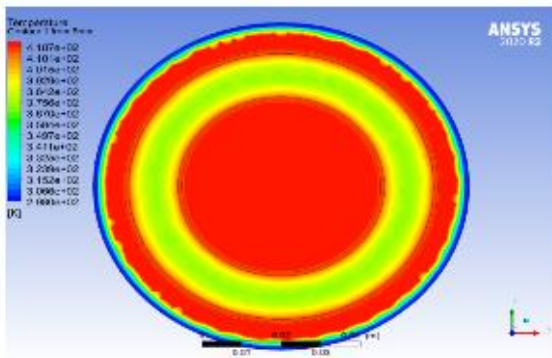
Fig 4: velocity contour



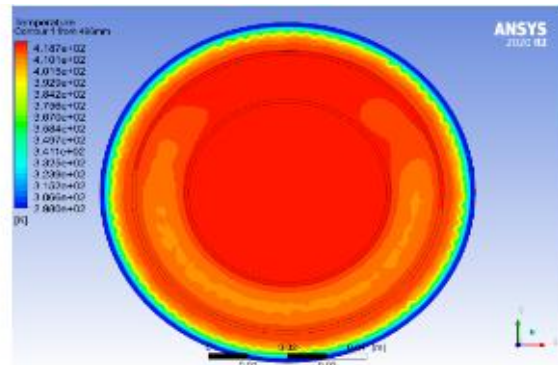
Temp contour, 2 mm from the starting end.



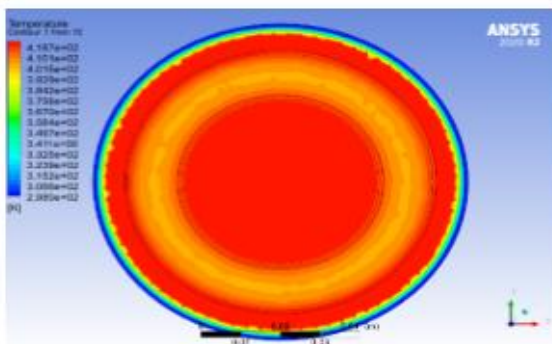
Temp contour, 495 mm from the starting end.



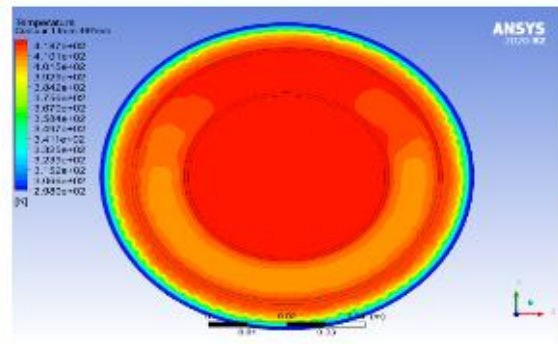
Temp contour, 5 mm from the starting end.



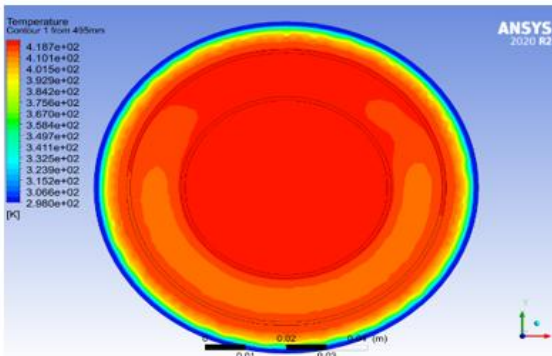
Temp contour, 496 mm from the starting end.



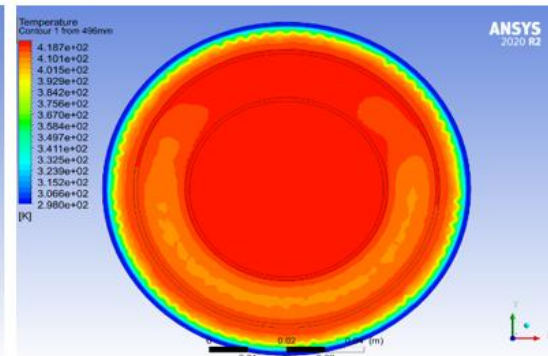
Temp contour, 10 mm from the starting end.



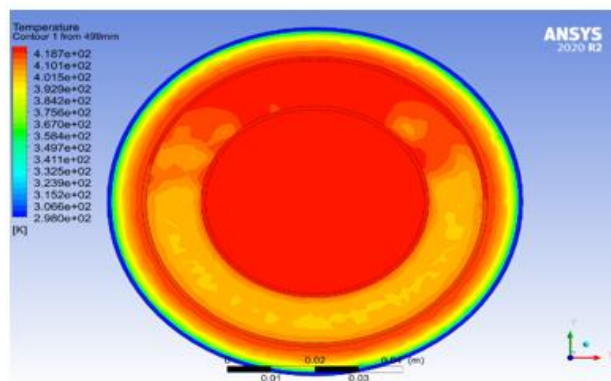
Temp contour, 497 mm from the starting end.



Temp contour, 498 mm from the starting end.



Temp contour, 499 mm from the starting end.



Temp contour, 500 mm from the starting end.

Fig 5: temperature contour of inner, intermediate & outer tube.

Table 3: Temperature data of Inner, Outer, and Intermediate tube with Liner and Radial distance.

| Tube linear Distance (mm) | Temp.                                | Tube radial distance from the centre of inner tube. (mm) | Oil inlet temp. (°C)      | Oil outlet temp. (°C)      | $\Delta T$ (Temp. Drop)           |
|---------------------------|--------------------------------------|--|---------------------------|----------------------------|-----------------------------------|
| 500                       | Constant.                            | 1  | 150                       | 150                        | 0                                 |
| 500                       | Constant.                            | 2  | 150                       | 150                        | 0                                 |
| 500                       | Constant.                            | 3  | 150                       | 150                        | 0                                 |
| 500                       | Constant.                            | 4  | 150                       | 150                        | 0                                 |
| 500                       | Constant.                            | 5  | 150                       | 150                        | 0                                 |
| 500                       | Constant.                            | 6  | 150                       | 150                        | 0                                 |
| 500                       | Constant.                            | 7  | 150                       | 150                        | 0                                 |
| 500                       | Constant till 280 mm                 | 8  | 150                       | 149.999                    | 0.001                             |
| 500                       | Constant till 280 mm                 | 9  | 150                       | 149.999                    | 0.001                             |
| 500                       | Constant till 220 mm                 | 10   | 150                       | 149.997                    | 0.003                             |
| 500                       | Constant till 220 mm                 | 11   | 150                       | 149.994                    | 0.006                             |
| 500                       | Constant till 170 mm                 | 12   | 150                       | 149.985                    | 0.015                             |
| 500                       | Constant till 110 mm                 | 13   | 150                       | 149.976                    | 0.024                             |
| 500                       | Constant till 60 mm                  | 14   | 150                       | 149.95                     | 0.05                              |
| 500                       | Constant till 60 mm                  | 15   | 150                       | 149.92                     | 0.08                              |
| 500                       | Constant till only 20mm tube length  | 16   | 150                       | 149.88                     | 0.12                              |
| 500                       | Constant till only 60 mm             | 17   | 150                       | 149.83                     | 0.17                              |
| 500                       | Less steep up to 60 mm               | 18   | 150                       | 149.76                     | 0.24                              |
| 500                       | Not constant                         | 19   | 150                       | 149.69                     | 0.31                              |
| 500                       | Not constant                         | 20   | 150                       | 149.6                      | 0.4                               |
| 500                       | Drop linearly up to 60 mm            | 21   | 150                       | 149.43                     | 0.57                              |
| 500                       | Drop linearly up to 60 mm            | 22   | 150                       | 149.3                      | 0.7                               |
| 500                       | Drop linearly up to 60 mm            | 23   | 150                       | 148.9                      | 1.1                               |
| 500                       | Drop linearly up to 60 mm            | 24   | 148.7                     | 148.4                      | 0.3                               |
| 500                       | Increase of surface temp up to 60 mm | 25 (inner surface of inner tube)                         | 150                       | 147.2                      | 2.8                               |
|                           | <b>PCM temp.</b>                     | <b>Intermediate tube (PCM)</b>                           | <b>PCM temp. at inlet</b> | <b>PCM temp. at outlet</b> | <b>Increments of temp. in PCM</b> |
| 500                       | Increase temp up to 60 mm            | 27   | 47                        | 132                        | 85                                |

|     |                           |                             |                        |                         |   |
|-----|---------------------------|-----------------------------|------------------------|-------------------------|---|
| 500 | Increase temp up to 60 mm | 28                          | 25                     | 125                     | 100                                       |
| 500 | Increase temp up to 60 mm | 32                          | 25                     | 125                     | 100                                       |
| 500 | Increase temp up to 60 mm | 37                          | 25                     | 132                     | 107                                       |
|     | <b>Temp.</b>              | <b>Outer tube (hot oil)</b> | <b>Oil inlet temp.</b> | <b>Oil outlet temp.</b> | <b><math>\Delta T</math> (Temp. Drop)</b> |
| 500 | Not constant              | 41.5                        | 149                    | 138                     | 11  |
| 500 | Not constant              | 42.5                        | 150                    | 134.5                   | 15.5                                      |
| 500 | Not constant              | 43.5                        | 142                    | 123                     | 19  |
| 500 | Not constant              | 44.5                        | 142                    | 123                     | 19  |
| 500 | Drop linearly up to 60 mm | 45.5                        | 121                    | 97                      | 24  |
| 500 | Drop linearly up to 60 mm | 46.5                        | 29.8                   | 28.1                    | 1.7                                       |

#### IV. Conclusion

The study commenced by conducting a comprehensive analysis of existing literature to ascertain the starting dimensions. Following this, the diameter and length of the energy storage system were computed using the energy requirements as the basis for the calculations. A geometric model of the energy storage system was constructed in the Design Modeller of Ansys Fluent Workbench, utilising the provided dimensions as a reference. Subsequently, the model was subjected to the meshing procedure using the Fluent Workbench, utilising the multizone meshing feature with a mesh size of 0.002 mm. The establishment of naming rules for the several constituents of the energy storage system, encompassing the input and outflow, was undertaken.

The simulation procedure involved the selection of parameters, such as double precision, the definition of materials, the specification of boundary conditions, and the utilisation of a pressure-based solver. The simulation was conducted under steady-state circumstances, with a duration of 1000 iterations.

The simulation yielded temperature contours for the Phase Change Material (PCM) within the intermediate tube, as well as temperature contours for the inner and outer tubes of the thermic fluid. These contours were generated based on their respective positions along the axis.

Upon completion of the simulation, it was noted that the temperature of the heated oil within the inner tube remained consistent within a radial distance of 7 mm along the whole length of the tube. Nevertheless, beyond the radial distance of 7 mm, the temperature demonstrates fluctuations along the length of the tube. TABLE 3 provides a vivid depiction of the non-uniform temperature distribution along the length of the tube as the radial distance from its centre grows. The temperature undergoes variations along the length of the tube, with the greatest impact found within the first 60 mm.

When the radial distance exceeds 25mm, specifically ranging from 27mm to 37.5mm, a section known as the intermediate tube section, the temperature distribution graph of the Phase Change Material (PCM) can be obtained at various radial positions. These positions include 27mm, 28mm, 32mm, and 37mm from the central axis of the tube. Significantly, it has been noted that the temperature distribution exhibits a high degree of similarity across all these places. The intermediate tube is filled with phase change material (PCM), erythritol, and because of the heating from both the inner tube and outside tube, the temperature of the PCM substance increases up to 60mm from its original temperature of 27°C. The observed rise in temperature is confined to the initial 60mm segment of the tube, attaining an approximate value of 152°C. After exceeding a length of 60mm, the temperature exhibits a consistent stability across all areas. This suggests that erythritol (PCM) exhibits effective

thermal energy absorption exclusively within the initial 60mm length, with no further absorption observed beyond this point.

When the radial distance exceeds 37.5mm, specifically within the range of 39.5mm to 46.5mm, referred to as the outer tube section, which is filled with heated oil, it becomes evident that the temperature of the oil is not uniformly maintained until a radial distance of 44.5mm. Currently, the temperature of the oil exhibits a consistent decline across the entirety of the tube's length. Like the phase change material (PCM), it is important to acknowledge that the effective thermal energy storage capacity of the PCM is constrained solely to the initial 60mm of tube length. This implies that because of heating from two opposing directions, the phase change material (PCM) is capable of efficiently retaining thermal energy alone within the initial 60mm segment of the tube.

Of the total length of the tube, which measures 500 mm, only the beginning segment spanning 60 mm is successfully employed for the purpose of storing and facilitating the passage of thermal energy between the heated oil and the Phase Change Material (PCM). The remaining 440 mm of the tube exhibits suboptimal efficacy in terms of thermal energy storage and transfer. The observed constraint can be ascribed to the velocity distribution of the heated oil flowing through the inner and outer tubes, which undergoes a transitional phase during the initial 60 mm of tube length.

Following the initial 60 mm, the velocity profile undergoes a transition into a developed phase, notably within the laminar zone. Once the flow reaches a state of complete development, the convective heat transfer coefficient (h) attains a constant value, resulting in a cessation of effective heat transmission. The presence of this trend is readily apparent based on the data provided in TABLE 3.

To optimise the thermal energy storage capacity of the Latent Heat Thermal Energy Storage (LHTES) system, it is advisable to include internal fins within the inner and intermediate tubes. The inclusion of fins in the system can improve heat transfer efficiency and increase the effective length of energy storage.

## 2. Scope of further research

The work presents substantial potential for future investigation. The use of the entire length of the tube, measuring 500 mm, in the research presents

a potential avenue for improving the thermal energy storage capacity of the proposed Latent Heat Thermal Energy Storage (LHTES) system. An area of potential enhancement lies in the integration of fins into the inner and intermediate tubes.

The inclusion of interior fins enables researchers to examine the effects of these elements on heat transport, energy storage, and system efficiency. The incorporation of internal fins within the LHTES system can augment heat transfer capabilities by expanding the accessible surface area for thermal exchange. Additionally, these fins can facilitate a more efficient dispersion of thermal energy throughout the system.

In addition, it is worth investigating the selection of materials for these fins, such as hybrid nanoparticles or alternative conductive substances, to enhance the thermal conductivity and energy storage capability of the system.

In general, the research can centre on examining the design, placement, and materials utilised in internal fins with the aim of optimising the performance and energy storage capacities of the LHTES system. This research endeavour has the potential to enhance the efficiency and effectiveness of thermal energy storage solutions across diverse applications, such as heating and cooling systems.

## References

- [1] WorldCoal Statistics - Worldometer
- [2] World Oil Statistics - Worldometer
- [3] WorldNatural Gas Statistics - Worldometer
- [4] Li, Zhi, Yiji Lu, Rui Huang, Jinwei Chang, Xiaonan Yu, Ruicheng Jiang, Xiaoli Yu, and Anthony Paul Roskilly. "Applications and technological challenges for heat recovery, storage and utilisation with latent thermal energy storage." *Applied Energy* 283 (2021): 116277.
- [5] Kaizawa, Akihide, Nobuhiro Maruoka, Atsushi Kawai, Hiroomi Kamano, Tetsuji Jozuka, Takeshi Senda, and Tomohiro Akiyama. "Thermophysical and heat transfer properties of phase change material candidate for waste heat transportation system." *Heat and mass transfer* 44 (2008): 763-769.
- [6] del Barrio, E. Palomo, A. Godin, M. Duquesne, J. Daranlot, J. Jolly, W. Alshaer, T. Kouadio, and A. Sommer. "Characterization of different sugar alcohols as phase change materials for thermal energy storage applications." *Solar Energy Materials and Solar Cells* 159 (2017): 560-569.

- [7] Kakiuchi, H., M. Yamazaki, M. Yabe, S. Chihara, and T. Terunuma. "Y. Sakata, T. Usami, A study of erythritol as phase change material, IEA Annex 10." In Proceedings of the Second PCMs and Chemical Reactions for Thermal Energy Storage Workshop, Chemical Engineering and Technology, Royal Institute of Technology, Sofia. 1998.
- [8] Zhang, Huaichen, Roel MJ van Wissen, Silvia V. Nedeá, and Camilo CM Rindt. "Characterization of sugar alcohols as seasonal heat storage media-experimental and theoretical investigations." In Advances in Thermal Energy Storage (EUROTHERM Seminar 99), May 28-30, 2014, Lleida, Spain. 2014.
- [9] Nomura, Takahiro, Masakatsu Tsubota, Teppei Oya, Noriyuki Okinaka, and Tomohiro Akiyama. "Heat storage in direct-contact heat exchanger with phase change material." *Applied thermal engineering* 50, no. 1 (2013): 26-34.
- [10] Agyenim, Francis, Philip Eames, and Mervyn Smyth. "Experimental study on the melting and solidification behaviour of a medium temperature phase change storage material (Erythritol) system augmented with fins to power a LiBr/H<sub>2</sub>O absorption cooling system." *Renewable energy* 36, no. 1 (2011): 108-117.
- [11] Mat, Sohif, Abduljalil A. Al-Abidi, Kamaruzzaman Sopian, Mohamad Yusof Sulaiman, and Abdulrahman Th Mohammad. "Enhance heat transfer for PCM melting in triplex tube with internal-external fins." *Energy conversion and management* 74 (2013): 223-236.
- [12] [hitechsolution.co.in/wpcontent/uploads/2018/11/hi-tech-therm-66.pdf](https://hitechsolution.co.in/wpcontent/uploads/2018/11/hi-tech-therm-66.pdf)
- [13] Ranjan, Rajeev, and Aseem C. Tiwari. "CFD Analysis of Latent Thermal Energy Storage for Erythritol Phase Change Material." (2021).
- [14] Honguntiker, P. V., and U. C. Pawar. "Characterization of erythritol as a phase change material." *IJSART* 5(2019):329-32.
- [15] <https://resources.systemanalysis.cadence.com/blog/msa2022-expressing-the-navier-stokes-equation-in-cylindrical-coordinate-systems>.
- [16] Amano, Ryoichi, and Bengt Sundén, eds. *Computational fluid dynamics and heat transfer: emerging topics*. Vol. 23. WIT Press, 2011.
- [17] Patankar, Suhas. *Numerical heat transfer and fluid flow*. Taylor & Francis, 2018.